Molecular Crystals and Liquid Crystals
Publication details, including instructions for authors and subscription information:
http://www.tandfonline.com/loi/gmcl16

Creation and Evolution of Excited States in α Particle Tracks in Anthracene Crystals

G. Klein [a]

[a] Centre de Recherches Nucleaires, Laboratoire de Physique des Rayonnements et d'Electronique Nucléaire, 23, rue du Loess, 67037, Strasbourg Cedex, France

Version of record first published: 19 Oct 2010.

To cite this article: G. Klein (1978): Creation and Evolution of Excited States in α Particle Tracks in Anthracene Crystals, Molecular Crystals and Liquid Crystals, 44:1-2, 125-149

To link to this article: http://dx.doi.org/10.1080/00268947808084974

Mol. Cryst. Liq. Cryst., 1978, Vol. 44, pp. 125–150

Printed in Holland

Creation and Evolution of Excited States in α Particle Tracks in Anthracene Crystals

G. KLEIN

Centre de Recherches Nucleaires, Laboratoire de Physique des Rayonnements et d'Electronique Nucléaire, 23, rue du Loess, 67037 Strasbourg Cedex, France

(*Received April 19, 1977*)

The kinematics of excited states in anthracene crystals bombarded by 5 MeV α particles is studied. The elementary processes which account for the transitions from the primary excited states to the lowest singlet S_1 and triplet T_1 excited states is described. The equations governing the evolution of the S_1 and T_1 excitons in the α particle track are then solved, and the scintillation decay curve is calculated. This calculated result is in good agreement with all available experimental results. The experimental part of this work are scintillation decay curves measurements. The scintillation decay was measured between 0.5 nsec and 40 μsec. The influence of the initial very fast singlet excitons quenching by triplet excitons can be seen in the beginning of the scintillation. The delayed component is described by the triplet exciton kinematics. The magnetic field effect on the scintillation was investigated. This effect is attributed to an effect on the $T_1 - T_1$ annihilation and an effect on the triplet excitons quenching by radicals which are formed in the α particle track.

The problem of creation and evolution of excited states in organic crystals bombarded by α particles is studied by analysing the radioluminescence: the intensity of the emitted light as a function of time, temperature, external magnetic field, and direction of the α particle.

An anthracene crystal bombarded by ionizing particles exhibits the same emission spectrum as the fluorescence spectrum which is attributed to the radiative transition from the first excited singlet state S_1 to the ground state S_0 ($S_1 \rightarrow S_0 + h\nu$). The formation of the S_1 excitons is a result of a sequence of elementary processes which we review in this paper. In a first stage (10^{-15} sec) the primary α particle and the secondary electrons are slowing down in the organic material and create excited states in a broad energy range at about 20 eV (excitons, plasmons, charge carriers). In a second stage, from 10^{-15} sec to 10^{-12} sec the absorbed energy is dissipated in the crystal and transformed into singlet (S_1) and triplet (T_1) excitons and phonons by non radiative transitions: electronic and vibrational relaxation, autoionization and charge carriers recombinations. In the third stage (10^{-12} sec to 10^{-5} sec) occurs the emission of light which can be studied experimentally in the range 10^{-9} sec to 10^{-5} sec. During this stage, also take place the diffusion of the excitons and bimolecular annihilations. The light emission of the singlet excitons resulting from the two first stages is the "prompt component" of the scintillation; its decay is not exponential, and extends over tens of nanoseconds; the light arising from singlet excitons created by annihilation of two triplets ($T_1 + T_1 \rightarrow S_1 + S_0$) is the "delayed component" and lasts microseconds.

In Section I we develop a kinetic study of the scintillation, as complete as possible, in which we use experimental and theoretical published results about the involved elementary processes.

Afterwards we present our experiments (Section II) which are measurements of the intensity of a scintillation as a function of time between 1 nsec and 40 μsec in various conditions of temperature and external magnetic field. These experimental results are discussed in Section III. The light intensity of the scintillation is calculated between 0 and 40 μsec and compared to our experimental results and other available data. The magnetic field effect have proven to be of great importance in understanding the details of the triplet exciton interactions and the creation of paramagnetic defects in α particle tracks.

I KINEMATICS OF EXCITED STATES IN α PARTICLE TRACKS

The earlier work about this problem has been summarized by Birks.[4,3] This problem was next studied by King and Voltz[1,2] and by Schott.[3] These authors showed the most important features but there were always difficulties to give a complete[1] or quantitative[3] study of this problem. A more complete analysis, including magnetic field effect experiments is given by Geacintov *et al.*[4]

I.1 Primary excited states

The passage of the primary α particle and the secondary electrons in the anthracene crystal results in the formation of various excited states.

The α particle and the high energy secondary electrons ($E \geq 100$ eV) lose energy by "optical collisions." Fast electrons energy loss spectra in thin crystals[2,5] show a broad absorption band at 20 eV which is attributed to the formation of plasmons. Their yield of formation is one plasmon for 25 eV[2]. Higher energy losses correspond to ionization and generation of electron-hole pairs. Thus, we conclude that the primary excited states generated by fast particles are plasmons and charge carriers.

The low energy secondary electrons ($E < 100$ eV) interactions with matter were less studied. In the following, we suppose that above the ionization potential (≈ 6 eV) the formation of plasmons still prevails. Secondary electrons with energies below 6 eV, and above the first singlet exciton energy (3.15 eV in anthracene) have a probability of 0.5 to create a singlet exciton. This can be seen from quantum yield measurements in anthracene crystals bombarded by very slow electrons.[6] Between the energies of the lowest triplet exciton T_1 and singlet S_1 an electron loses its energy by the formation of triplet excitons.[2] The matrix elements for such transitions involve exchange integrals, therefore they are generally one order of magnitude smaller than those corresponding to allowed transitions ($S_0 \rightarrow S_1$ for example). However, this electronic transition ($S_0 \rightarrow T_1$) seems to be more likely than the intramolecular vibration excitation: In anthracene crystals excited by photons at 10 eV, 30 per cent of the initial singlet excitons undergo autoionization followed by the formation of a triplet exciton by the emitted electron

if its kinetic energy is more than the triplet energy.[7] The exciton formation by secondary electron collisions corresponds to a very narrow energy range (1.8 eV to 6 eV), but it is important because of the large number of secondary electrons having these energies.

Thus, the primary excited states in α particle tracks are principally plasmons, excitons T_1, S_1, S_2, charge carriers and few intramolecular vibrational excitations. As the energy necessary for the formation of a plasmon is 25 eV, and less for excitons and charge carrier pairs, and neglecting vibrational excitations, we assume that an average energy of 25 eV is necessary for the creation of one primary excited state.

A 5 MeV α particle track is roughly of cylindrical symmetry. Secondary electrons of energies less than 500 eV correspond to 90 per cent of the initial α particle energy.[3] The average value of the range of these secondary electrons is roughly 100 Å (150 Å for 500 eV). Therefore, we suppose that 100 Å is a good approximation for the α particle track radius r_0.

I.2 Non-radiative transitions

The plasmon lifetime calculated from the linewidth of the broad absorption band is between 10^{-15} sec and 10^{-16} sec.[2,5] At these high energies ($\approx$20 eV) the most important decay process is autoionization.[8,9] The resulting secondary electrons have often enough kinetic energy to form triplet T_1 or singlet S_1, S_2 excitons (see Section I.1). Thus, for each plasmon, we get one charge carrier pair and often one S_1 or T_1 exciton. Because of the very short lifetime of the plasmons we neglect their interactions with other plasmons or charge carriers. We conclude that after 10^{-15} sec only remains S_1 and T_1 excitons and charge carriers.

The charge carrier recombination will take place in the next time scale: 10^{-13} sec to 10^{-12} sec. The concentration of charge carriers in the α particle track is about $n_+ = n_- \approx 10^{19}$ cm^{-3} (see Section III.1.1 and Ref. 3) and the bimolecular electron-hole recombination rate constant is $\gamma_{+-} = 10^{-6}$ cm^3 sec^{-1};[10] thus, the recombination rate constant is $n_+\gamma_{+-} = 10^{13}$ sec^{-1}. The electrons produced by ionization, or autoionization are thermalized at a distance from the hole of 50 Å or more.[11] This distance is larger than the average distance between two ions in the track. Therefore, electrons recombination with holes without any spin correlation results in the formation of 25 per cent singlet and 75 per cent triplet excitons.[3]

Singlet or triplet excitons quenching by charge carriers is negligible compared to electron-hole recombination: the bimolecular annihilation rate constant of triplets by free electrons or holes is $\gamma_{T+} \approx \gamma_{T-} \approx 10^{-9}$ cm^3 sec^{-1} $\ll \gamma_{+-}$.[12] And the quenching rate constant of singlets by trapped holes or electrons is 10^{-8} cm^3 sec^{-1} $\ll \gamma_{+-}$.[13]

Assuming that no other important non radiative quenching processes were omitted, we conclude that at the end of this second stage ($\approx 10^{-12}$ sec), the α particle track is made of triplet T_1 and singlet S_1 excitons which yield of formation is about one exciton for 25 eV. The triplet excitons formation is promoted by ions recombinations, whereas direct excitation results in the formation of more singlet excitons. The actual efficiency of these processes is not known, but it seems reasonable to suppose that the numbers of triplet and singlet excitons are roughly equal.

The creation of defects by photochemical processes in irradiated organic materials is a well established phenomenon.[4,8,14–16] It was shown by Fuchs *et al.*[8] that in liquid benzene photochemical processes are very efficient in the second (S_2) and third (S_3) singlet excited states. This results in a decrease of the fluorescence quantum yield. At energies higher than the ionization potential, this phenomenon decreases rapidly, because it is in competition with autoionization, which is a faster process. In organic crystals, like anthracene, the defect production occurs surely in the same manner, but with smaller efficiencies; indeed, the fluorescence quantum yield is approximately independent of the excitation energy.[17] However, these permanent defects in anthracene cannot be neglected because of their quenching effect on the long lived triplet excitons: the triplet exciton lifetime before X ray irradiation of 22 msec decreases to a value of 1.5 msec after dose of 4×10^3 rad.[14] This is to be compared to the α particle track where the locally deposited dose is of the order of 10^7 rad (see Section III.1.2). These defects were not taken into account in the scintillation analysis of King and Voltz[1] and Schott;[3] their quenching effect on singlet excitons in tetracene were studied by Geacintov *et al.*[4]

An external magnetic field has no effect on the singlet or triplet excitons population in this time range (10^{-13} sec to 10^{-12} sec). The most important reactions which possibly could be magnetic field sensitive are:

$$\begin{array}{l} e^* + S_0 \rightarrow (e, T_1) \rightarrow e + T_1 \\ e + S_0 \longleftarrow \end{array} \qquad (1)$$

$$\begin{array}{l} e + S_1 \rightarrow (e, T_1) \rightarrow e + T_1 \\ e + S_0 \longleftarrow \end{array} \qquad (2)$$

$$\begin{array}{l} e + T_1 \rightarrow (e, T_1) \rightarrow e + T_1 \\ e + S_0 \longleftarrow \end{array} \qquad (3)$$

$$\begin{array}{l} S_n \rightarrow e^* + h \rightarrow e + T_1 + h \rightarrow (T_1, T_1) \rightarrow T_1 + T_1 \\ \qquad\qquad\qquad\qquad\qquad\qquad S_0 + S_1 \longleftarrow \end{array} \qquad (4)$$

where e, h mean thermalized electron and hole, e^* is an electron with kinetic

energy, and the arrows correspond to spin conserving transitions. The triplet–triplet fusion, and the triplet quenching by paramagnetic defects will be studied in the next paragraph (Section I,3). The spin state of the pairs (e, T_1) and (T_1, T_1) changes coherently with time because of the triplet fine structure interaction, which can be modulated by a magnetic field. Thus, the reverse processes are magnetic field dependent.[19] However, in α particle tracks, in reactions (1), (2) and (3), the free electron and the pair state lifetimes are very short, so that coherent spin states mixing cannot occur, and there is no magnetic field effect.[19] The reaction (4) is impossible in α particle tracks because electron-hole geminate recombination is scarce;† a random recombination produces triplet excitons with no correlated spin states.

I.3 Kinematics of singlet S_1 and triplet T_1 excitons

The singlet and triplet excitons can diffuse out of the α particle track; the corresponding diffusion coefficients are D_S and D_T. Because of this motion, the excitons can also disappear by bimolecular annihilation. The most important reactions are:

$$S_1 \xrightarrow{k_S} S_0 + h\nu \rightarrow S_1 \cdots \rightarrow S_0 + h\nu \qquad (5)$$

$$S_1 + S_1 \xrightarrow{\gamma_{SS}} S_0 + S_n \rightarrow S_0 + S_1 \qquad (6)$$

$$S_1 + T_1 \xrightarrow{\gamma_{ST}} S_0 + T_n \rightarrow S_0 + T_1 \qquad (7)$$

$$T_1 + T_1 \xrightarrow{\gamma_S} S_0 + S_1 \qquad (8)$$

$$T_1 + T_1 \xrightarrow{\gamma_T} S_0 + T_n \rightarrow S_0 + T_1 \qquad (9)$$

$$T_1 + R \xrightarrow{\gamma_R} S_0 + R \qquad (10)$$

where $2\gamma_S + \gamma_T = \gamma_{TT}$. The reaction (5) is the fluorescence and the self-absorption which is important in anthracene crystals. The reactions (6–9) are fusions which result in the disappearance of one exciton. The last one (10) is the quenching of a triplet exciton by a defect arising from photochemical processes. Some of these defects have a doublet character (spin $\frac{1}{2}$). γ_S and γ_R are the only parameter which are magnetic field dependent and they were widely studied.[14,15,20] Geacintov *et al.*[4] studied the consequence of this magnetic field effect on scintillation. The parameters D_T,[21] D_S,[22] γ_{SS},[23,24]

† This reaction is possible with U.V. light or β particle irradiation, where isolated highly excited states are created.[7,18] In this case the triplet production is magnetic field sensitive, like in fission experiments.

TABLE I

Parameter values governing the creation and evolution of excited states in 5.3 MeV α particle tracks in anthracene crystals.

A Values measured independently of this work, or calculated, or estimated.

B Values which give the best fit between the calculated scintillation light intensity and the corresponding experimental results, including magnetic field effect.

Parameter	A	B
D_T ($cm^2\ sec^{-1}$) in the (ab) plane	2×10^{-4}	2×10^{-4}
D_S ($cm^2\ sec^{-1}$)	5×10^{-3}	5×10^{-3}
γ_{SS} ($cm^3\ sec^{-1}$)	10^{-8}	1.5×10^{-8}
γ_{ST} ($cm^3\ sec^{-1}$)	5×10^{-9}	2×10^{-9}
γ_{TT} ($cm^3\ sec^{-1}$)	2×10^{-11}	3.4×10^{-11}
γ_S/γ_{TT}	0.18	0.22
k_S (sec^{-1})	2×10^8	2×10^8
k'_S (sec^{-1})	4×10^7	4×10^7
r_0 (Å)	100	100
$n_S(0, 0)(cm^{-3})$	10^{19}	10^{19}
$n_T(0, 0)(cm^{-3})$	10^{19}	1.4×10^{19}
$\gamma_R n_{R0}(sec^{-1})$	10^7	4×10^7

γ_{ST},[23,24] γ_{TT},[25] γ_S/γ_{TT},[26] k_S[27] were determined experimentally, independently of this work and are reported in Table IA. k'_S depends on the crystal size; in our case we measured it by β particle excitation.

In anthracene crystals, intersystem crossing ($S_1 \rightarrow T_1$) and internal conversion ($S_1 \rightarrow S_0$) are neglected. This means that we suppose that the fluorescence quantum yield is equal to unity.[17] In the time range we studied (1 nsec to 40 μsec) the monomolecular decay of triplet excitons may be neglected (rate constant: 40 sec^{-1}).

The concentrations of triplet excitons $n_T(\mathbf{r}, t)$ and singlet excitons $n_S(\mathbf{r}, t)$ are functions of space ($\mathbf{r}$) and time (t); they are given by the equations:

$$\frac{\partial n_T(\mathbf{r}, t)}{\partial t} = D_T \nabla^2 n_T - \gamma_{TT} n_T^2 - \gamma_R n_R(\mathbf{r}, t) n_T \tag{11}$$

$$\frac{\partial n_S(\mathbf{r}, t)}{\partial t} = D_S \nabla^2 n_S - \gamma_{SS} n_S^2 - \gamma_{ST} n_S n_T - k_S n_S + \gamma_S n_T^2 \tag{12}$$

The concentration of quenchers $n_R(\mathbf{r}, t)$ and the initial conditions $n_T(\mathbf{r}, 0)$, $n_S(\mathbf{r}, 0)$ will be studied later (Section III.1.1 and III.1.2). In Eq. (12) the monomolecular singlet decay is taken into account by $-k_S n_S$, where $1/k_S$

is the singlet S_1 lifetime without self-absorption. The range of the emitted photons in the crystal is 10^{-4} cm or more, corresponding to an absorption coefficient of 10^4 cm^{-1} or less.[28] Therefore, these emitted photons escape from the track whose radius is initially 100 Å, but they do not escape necessarily from the crystal: 80 per cent of them are absorbed again out of the track, where bimolecular quenching cannot occur. We distinguish between the singlets of the track, which number is $N_S(t)$ and the $N'_S(t)$ singlets which are out of the track. They are correlated by the equation:

$$\frac{dN'_S(t)}{dt} = (1 - k'_S/k_S)k_S N_S - k'_S N'_S \tag{13}$$

with the initial condition $N'_S(0) = 0$.

Knowing the initial conditions $n_S(\mathbf{r}, 0)$, $n_T(\mathbf{r}, 0)$ and $n_R(\mathbf{r}, t)$, the concentrations $n_S(\mathbf{r}, t)$ can be calculated by solving Eqs. (11) and (12). $N_S(t)$ is obtained by integration of $n_S(\mathbf{r}, t)$. $N'_S(t)$ is then given by Eq. (13), and the light intensity of the sintillation is:

$$i(t) = k'_S(N_S(t) + N'_S(t))$$

The part of $i(t)$ corresponding to the singlet excitations created by direct excitation or by electron-hole recombination is the "prompt component" of the scintillation, and the part originating from triplet–triplet annihilation ($\gamma_S n_T^2$) is the "delayed component".

II EXPERIMENTAL

The time dependence of the light intensity of the scintillation was measured in three parts: the very beginning of the scintillation $i(t)$ is studied in Section II.1 in the time range 0.5 nsec to 20 nsec; we tried to show the competition between the diffusion of the singlet excitons out of the track and their quenching by triplet or other singlet excitons. In Section II.2 were studied longer times, from 10 nsec to 40 μsec, where triplet–triplet annihilation is important. The last part, Section II.3 deals with magnetic field effects which give informations about triplet–triplet and triplet–doublet interactions in α particle tracks.

II.1 Measurements of the beginning of the scintillation

The scintillation decay curve was measured, using the single photoelectron sampling method.[29] The experimental set-up is reported in Figure 1. The anthracene crystal bombarded by 5.3 MeV α particles of a ^{210}Po radioactive source, is placed upon the photocathode of a photomultiplier PM1 (Dario 56

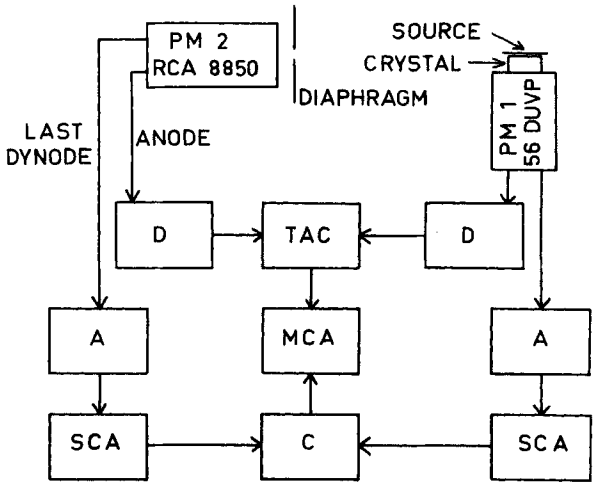

FIGURE 1 Experimental arrangement used to measure fast scintillation decay curves. PM—photomultiplier; D—fast discriminator; TAC—time to amplitude converter; MCA—multichannel analyser; A—amplifier; SCA—single channel analyser; C—slow coincidence circuit.

DUVP). The following discriminator triggered by the beginning of the PM1 signal gives the zero-time signal corresponding to the passage of the α particle. A second photomultiplier PM2 (RCA 8850) is diaphragmed, so that on an average one photoelectron per scintillation is formed at its photocathode and generates the delayed timing pulse. The time intervals between the output signals of the two discriminators are measured by a time to pulse height converter TAC (Chronetics Model 105) and analysed and stored by a multichannel analyzer MCA. A slow coincidence circuit, gating the MCA was used to select constant pulse heights in order to decrease the time jitter of the triggering of the discriminators and get a better time resolution (≤ 1 nsec). Moreover, on PM2, pulse heights corresponding to one photoelectron were selected: in this case, for each scintillation, the probability that a photon is detected by PM2 at time t is proportional to $i(t)$. Thus, the curve registered in the MCA is proportional to $i(t)$.

The anthracene crystal was grown from the melt from zone refined anthracene (Merck Art. 1454). The crystal was cleaved along the (a, b) plane (2 mm thick) and was washed in xylene before the experiment to avoid surface quenching of excitons. The α radioactive source is placed upon the (a, b) face of the crystal, so that the mean direction of the α particles is perpendicular to the (a, b) plane. With this geometry, all the analysed photons have to pass through the crystal, so that self-absorption is the same for all these photons and can be easily calculated (see Section I.3).

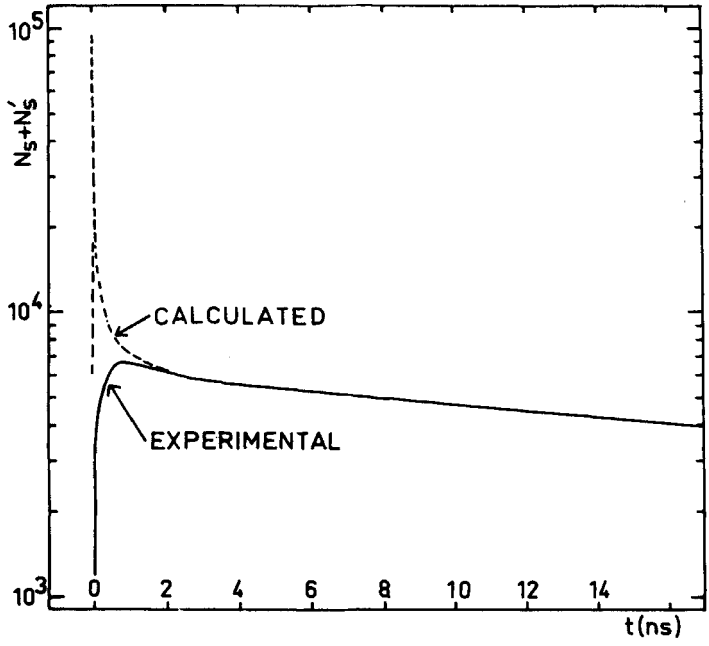

FIGURE 2 Time dependence of the number of singlet excitons $N_S(t) + N'_S(t)$ in an anthracene crystal bombarded by a 5.3 MeV α particle perpendicularly to the crystal (a, b) plane.

On Figure 2 is reported the scintillation decay curve $i(t)$. The 1 nsec rise time (10 per cent to 90 percent of the maximum) is that corresponding to the apparatus; no real scintillation rise time could be measured. This implies that S_1 excitons are formed in less than 0.5 nsec, which is in agreement with Section I where it was shown that S_1 excitons are produced in 10^{-12} sec or less. The decay of $i(t)$ is not exponential. In the very beginning of the decay the apparent lifetime of the singlet excitons is 20 nsec which is less than the isolated singlet exciton lifetime (25 nsec). This implies that S_1 excitons disappear not only by monomolecular radiative decay. This initial quenching is more striking in naphtalene crystals (see Figure 3): $i(t)$ was measured in the same experimental conditions as those used for anthracene.† The corresponding apparent S_1 exciton lifetime in the very beginning of the scintillation is 10 nsec, whereas the isolated S_1 exciton lifetime measured by U.V. or β particle irradiation is 115 nsec.

† The risetime, or time resolution are worse for naphtalene than for anthracene, because in the case of naphtalene, the light intensity is weaker. This results in fluctuations in the build-up of the PM1 signal and time jitter of the zero-time signal.

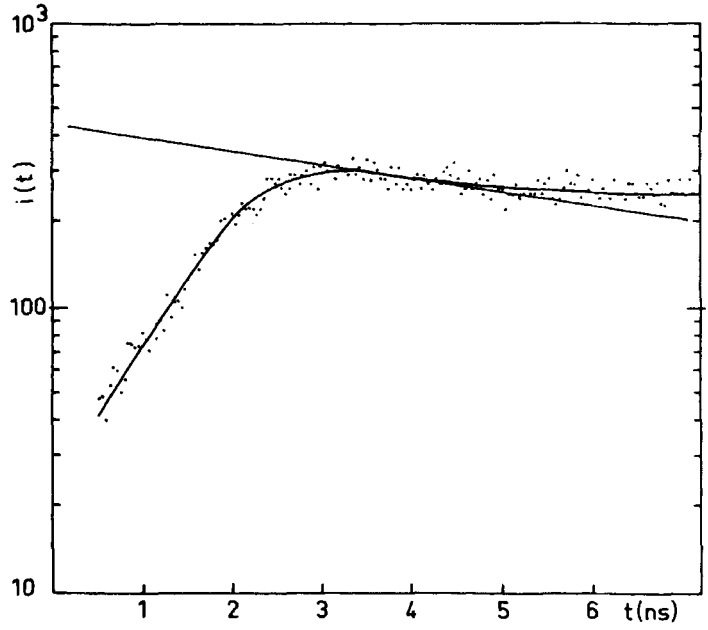

FIGURE 3 Scintillation decay curve of a naphtalene crystal bombarded by 5.3 MeV α particles.

II.2 Measurements of the delayed component of the scintillation between 10 nsec and 40 μsec

The light intensity decay $i(t)$ was measured between 10 nsec and 40 μsec using the experimental set-up shown in Figure 4.† The same single photoelectron method was used. PM2 was a low noise photomultiplier (Dario 56 DUVP). The time intervals Δt between the PM1 and PM2 signals were measured by a bistable which is opened by the PM1 signal and closed by the PM2 signal. The resulting rectangular pulses, which widths are Δt were modulated by a $f = 100$ MHz sinusoidal oscillator. The number of periods $f\Delta t$ were counted by a binary scaler "SEN type 194." This result is stored in a memory of 4096 channels "Intertechnique BM 96" at the corresponding address. Thus, the scintillation decay curve of the anthracene crystal bombarded by 5.3 MeV α particles is given with 10 nsec ($= 1/f$) per channel over a time range of 40.96 μsec: see Figure 5.

The temperature dependence of the scintillation decay curves of anthracene crystals bombarded by 5.3 MeV α particles was measured, using a cryostat and the same electronic apparatus. Compared to the scintillation decay

† The electronic part was carried out by MIEHE, OSTERTAG and GEIST.

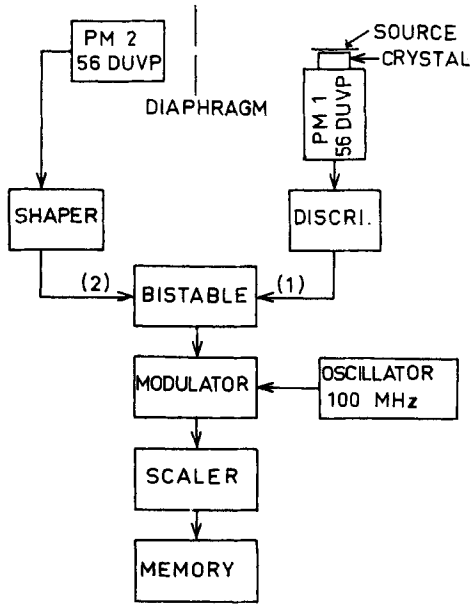

FIGURE 4 Experimental apparatus used to measure slow scintillation decay curves.

curve at room temperature, at 80 K the initial decay is faster, but there is no change in the slope after 0.3 μsec. The integrated light intensities in the time intervals 0 to 40 μsec, and 0.3 μsec to 40 μsec at different temperatures are reported in the Figure 6.

II.3 Magnetic field effects

The same single photoelectron and delayed coincidence methods were used to measure the magnetic field effects on the scintillation decay curves (Figure 7). The same α particle source was used. The measurements were performed alternatively with and without magnetic field during periods of 10 sec; the corresponding results were stored in two different parts of the MCA memory. During the time interval 5 sec, between two measurements the magnetic field was sitched on (or off) and the corresponding part of the MCA memory was selected. This sequence of operations was monitored by an external clock. The (a, b) face of the anthracene crystal was glued to a plexiglass cylindrical light pipe, which could be rotated around his axis, so that the fixed magnetic field direction could be oriented in the crystal (a, b) plane. The other end of the light pipe is in good optical contact with the PM1 photocathode. The PM1 and PM2 photocathodes were respectively at 15 cm and

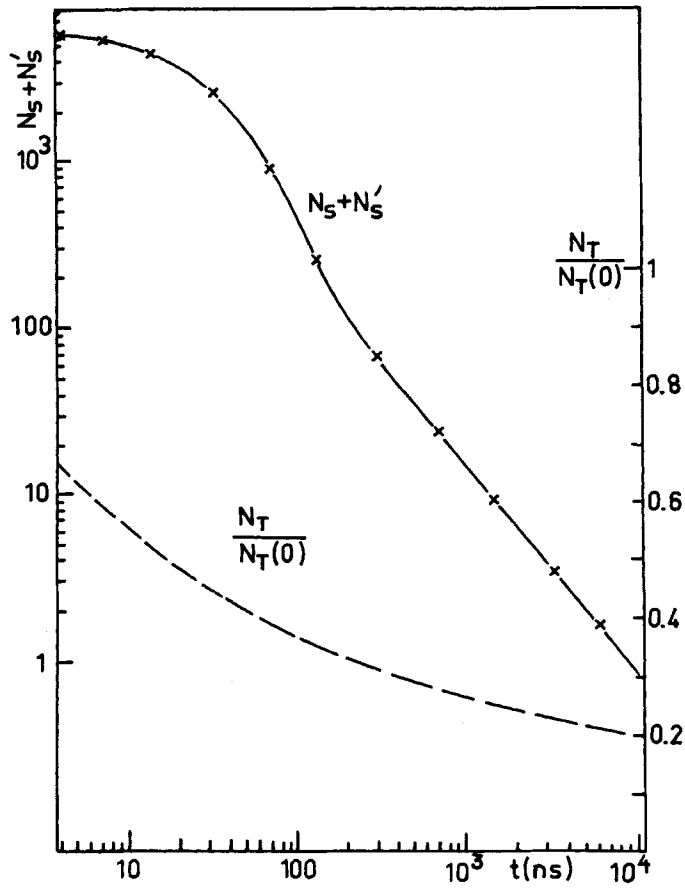

FIGURE 5 Time dependence of the number of singlet excitons, $N_S(t) + N'_S(t)$, in an anthracene crystal excited by a 5.3 MeV α particle. Full line: experimental result; crosses: calculated values. The lower broken line shows the relative variations of the number of triplet excitons.

50 cm from the crystal and shielded from stray magnetic fields. The number of scintillations detected by PM1 was almost independent of the magnetic field and the average number of coincidences per scintillation was less than 0.1. In these conditions the magnetic field effect on the number of coincidences stored in the MCA is equal to the effect on the light intensity $i(t)$.

We measured the relative variation of the light intensities upon magnetic field application: $\Delta i/i = (i_H(t) - i_0(t))/i_0(t)$ where the subscripts H and 0 correspond to measurements with and without magnetic field. We measured that $\Delta i/i$ is nearly independent of time; therefore, only the variations of the integrated intensities $\Delta i_p/i_p$ between 0 and 80 nsec, and $\Delta i_d/i_d$ between 0.7

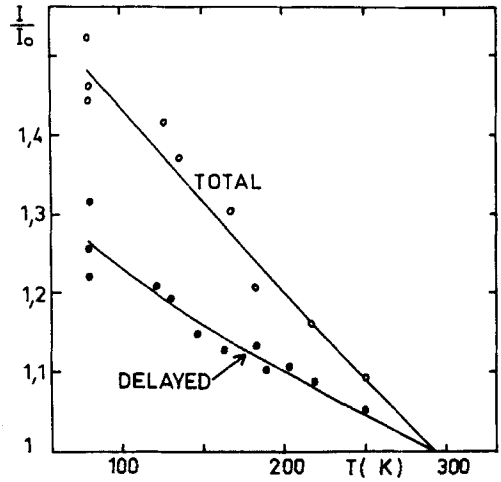

FIGURE 6 Temperature dependence of the integrated light intensity of anthracene crystals bombarded by 5.3 MeV α particles. Open circles: integration between 0 and 40 μsec; closed circles: integration between 0.3 μsec and 40 μsec.

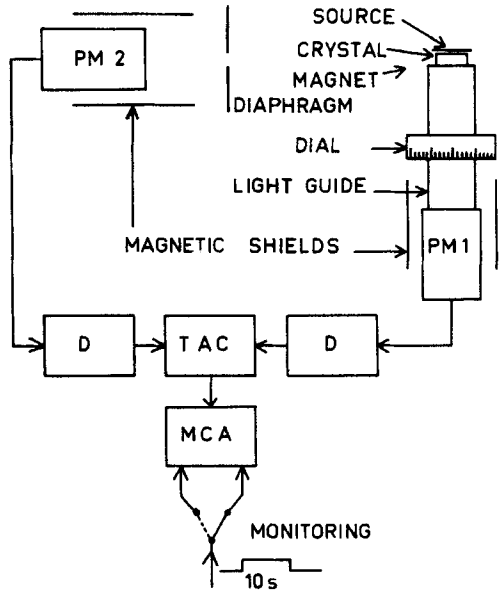

FIGURE 7 Experimental apparatus used to measure the magnetic field dependence of the scintillation decay. The abbreviations are the same as in Figure 1.

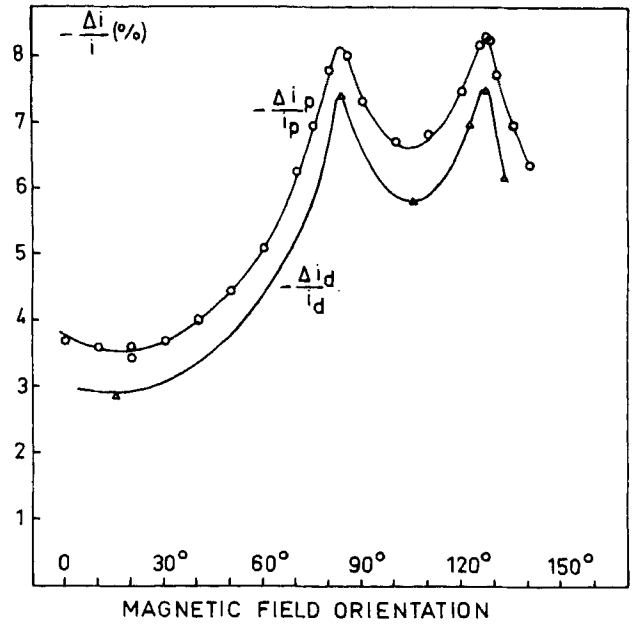

FIGURE 8 Relative variations of the integrated light intensities of anthracene crystals excited by 5.3 MeV α particles as a function of the orientation of the magnetic field in the crystal (*a*, *b*) plane. The magnetic field intensity was 4000 Gauss. $\Delta i_p/i_p$: integration between 0 and 80 nsec. $\Delta i_d/i_d$: integration between 0.7 μsec and 10 μsec.

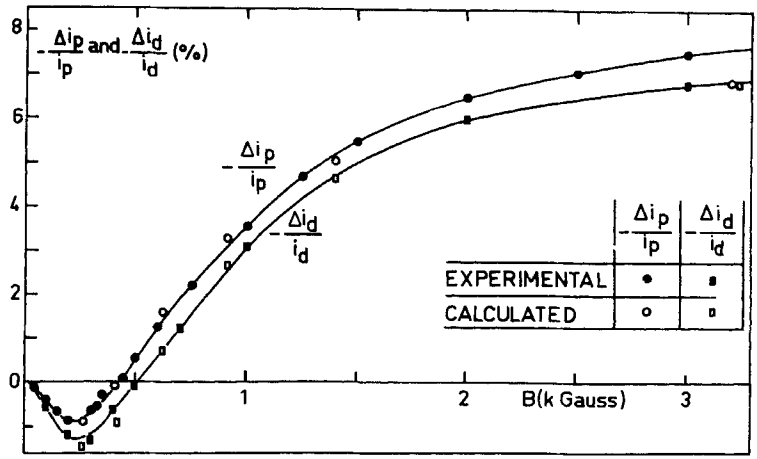

FIGURE 9 Relative variations of the integrated light intensities of anthracene crystals excited by 5.3 MeV α particles as a function of the magnetic field intensity. The magnetic field is in a resonance direction. $\Delta i_p/i_p$: integration between 0 and 80 nsec. $\Delta i_d/i_d$: integration between 0.7 μsec and 10 μsec.

and 10 μsec were studied. The anisotropies of $\Delta i_p/i_p$ and $\Delta i_d/i_d$ as a function of the magnetic field orientation in the crystal (a, b) plane are reported in Figure 8 for a magnetic field strength of 4000 Gauss. The influence of the magnetic field strength is shown in Figure 9, where the magnetic field was in a resonance direction of the (a, b) plane ($H_\Lambda b = 23°$).

III DISCUSSION

The scintillation analyses of King and Voltz[1] or Schott[3] can explain the main experimental features about the scintillation, but the three Eqs. (11), (12) and (13) governing the excitons evolution were never solved completely. In the first analysis, the singlet exciton quenching by triplet or singlet excitons was neglected, and in the second one the resolution of the equations were only qualitative. The paramagnetic defects formation by irradiation and their quenching effect on triplet excitons was widely studied[14–16 4] but was never taken into account in the kinematics of the scintillation. In this paper, Eq. (11) was solved analytically and Eqs. (12) and (13) were solved numerically. These results were fitted to all known experimental results. This discussion was limited to the problem of 5.3 MeV α particle tracks in anthracene crystals because for this problem enough data are available to solve it theoretically with good accuracy. Only in these conditions will the comparison with the experimental results be relevant.

III.1 Calculation of the scintillation decay curves

III.1.1 Initial exciton concentrations The initial concentrations of triplet excitons $n_T(\mathbf{r}, 0)$ and singlet excitons $n_S(\mathbf{r}, 0)$ are assumed to be of cylindrical symmetry and gaussian functions of the distance ($r \equiv |\mathbf{r}|$) to the center of the track. The axis which is the α particle path will be perpendicular to the (a, b) plane. Moreover, n_T and n_S are supposed to be constant all along the α particle track. This latter assumption is partly wrong, because the linear energy transfer (LET) increases from the beginning to the end of the α particle path. However, this does not change significantly our results for two reasons: firstly because the experimental shape of the scintillation decay curves $i(t)$ is nearly independent of the α particle energy.[30] The second reason is that the integrated intensity of scintillation per path length changes only slowly with the LET of the α particle.[3,31] Thus, n_S and n_T are given by:

$$n_S(r, 0) = n_S(0, 0)\exp(-r^2/r_0^2) \tag{14}$$

$$n_T(r, 0) = n_T(0, 0)\exp(-r^2/r_0^2) \tag{15}$$

where r_0 is the "track radius" which will be taken 100 Å (see I.1). $n_S(0, 0)$ and $n_T(0, 0)$ are the initial concentrations at time zero, at the center of the track; they are related to the total initial numbers of S_1 excitons $N_S(0)$ and T_1 excitons $N_T(0)$ by:

$$N_S(0) = \pi r_0^2 l n_S(0, 0) \tag{16}$$

$$N_T(0) = \pi r_0^2 l n_T(0, 0) \tag{17}$$

where l is the α particle path length. In anthracene crystals, for 5.3 MeV α particles $l = 30\ \mu$.[32] As stated above (Section I.2) the yield of formation of the excitons S_1 and T_1 are equal, and 1 exciton for 25 eV, i.e. $N_S(0) + N_T(0) = 2.1 \times 10^5$ excitons and $N_S(0)/N_T(0) \approx 1$. This is equivalent to:

$$n_S(0, 0) \approx n_T(0, 0) \approx 10^{19}\ \text{cm}^{-3}$$

III.1.2 Concentration of the triplet excitons quenching centers It was shown in Section I.2 how triplet quenching centers can be formed by photochemical processes in irradiated crystals. Most of them are chemical defects or radicals and have a doublet (spin $\frac{1}{2}$) character. The energies of most primary excited states are far above the ionization potential. In this energy range the photochemical processes are negligible compared to autoionization. It is known that the yield of radical formation increases with the LET and is related to a bimolecular interaction between two excited states.[16] Further, it can be seen that these interactions probably are $S_1 - S_1$ or $S_1 - T_1$ interactions (Eqs. (6) and (7)) which increase with LET and result in the formation of singlet (S_n) or triplet (T_n) excitons whose energy is near the ionization potential, where the photochemical processes are the most efficient.[8] In the following parts of this discussion, it is shown that the concentrations of the excitons quenching defects are not important compared to $n_S(0, 0)$ and $n_T(0, 0)$ and that two time intervals may be distinguished. During the first one from zero to 1 nsec the defects are produced, and the quenching of singlet and triplet excitons by the defects is neglected compared to the quenching by other singlet or triplet excitons. During the second one (1 nsec to 40 μsec) the defects production is negligible and the quenching of triplet excitons becomes operative. Therefore, in Eq. (11) it may be supposed that the defects concentration is independent of the time and has the same shape and symmetry as $n_S(r, 0)$ or $n_T(r, 0)$:

$$n_R(\mathbf{r}, t) = n_R(r) = n_{R0} \exp(-r^2/r_0^2) \tag{18}$$

where n_{R0} is the concentration at the center of the track.

The quenching rate constant $\gamma_R n_{R0}$ of the T_1 excitons by radicals may be calculated approximately: Ern and McGhie[15] measured that in an anthracene crystal irradiated by electrons emitted by tritium, $\gamma_R n_{R0}$ is 1.5×10^{-3}

$\sec^{-1}$ for 1 erg of β particle energy absorbed per gram of anthracene crystal. The volume of a 5.3 MeV α particle track is $\pi r_0^2 l = 10^{-14}$ cm^3 (with $l = 30\ \mu$ and $r_0 = 100$ Å). Taking a density of 1.25 g cm^{-3}, its mass will be 1.2×10^{-14} g. The deposited energy in the track is 5.3 MeV, which corresponds to a dosage of 7×10^8 ergs/g and a value of $\gamma_R n_{R0} \approx 10^6$ sec^{-1}. However, the radical production yield for 5 MeV α particles is about 10 times larger than for electrons.[16] Therefore, in our case, the true value of $\gamma_R n_{R0}$ will be 10 times larger than the previously calculated value: $\gamma_R n_{R0} \approx 10^7$ sec^{-1}.

This value of $\gamma_R n_{R0}$ and the values of r_0, $n_T(0, 0)$, $n_S(0, 0)$ calculated in Section III.1.1 are reported in Table IA.

III.1.3 Resolution of equation (11) governing the triplet excitons evolution

$$\frac{\partial n_T(r, t)}{\partial t} = D_T \nabla^2 n_T(r, t) - \gamma_{TT} n_T^2(r, t) - \gamma_R n_R(r) n_T(r, t) \qquad (19)$$

The initial conditions $n_T(r, 0)$, $\gamma_R n_R(r)$ were determined previously, and the parameters are given in Table IA. To solve this equation, we make some approximations which correspond to our experimental conditions: it will be supposed that the track is of cylindrical symmetry at all times, i.e., that its axis is perpendicular to the crystal (a, b) plane, and that the excitons diffusion is isotropic in the (a, b) plane.

The triplet excitons evolution can be characterized by 3 time constants: $t_a = r_0^2/4D_T$ for the diffusion of the triplet excitons perpendicularly to the track axis, $t_b = 1/(n_T(0, 0)\gamma_{TT})$ for the $T_1 - T_1$ bimolecular annihilation, $t_c = 1/(n_{R0}\gamma_R)$ for the triplet excitons quenching by radicals. Using the parameter values of Table IA one obtains $A = t_a/2t_b \approx 0.12$ and $B = t_a/t_c \approx 1.2 \times 10^{-2}$. In these conditions ($A \leq 1$ and $B \leq 1$), the Eq. (19) can be solved analytically by the prescribed diffusion method:[33] according to this method, the distribution of triplet excitons $n_T(r, t)$ remains a gaussian function of r at all times:

$$n_T(r, t) = g(t) \frac{n_T(0, 0)}{1 + t/t_a} \exp\left[- \frac{r^2}{r_0^2(1 + t/t_a)} \right]$$

The function of time $g(t)$ can be calculated by replacing $n_T(r, t)$ by this expression in Eq. (19), multiplying each member by $2\pi r dr$, and integrating from $r = 0$ to infinity one obtains:

$$\frac{dg}{dt} = -g^2 \frac{t_a}{2t_b(t + t_a)} - g \frac{t_a}{t_c(t + 2t_a)}$$

If $A < 1$ and $B \ll 1$, this equation is equivalent to:

$$\frac{dg}{dt} = (-Ag^2 - Bg) \frac{1}{t + t_a}$$

By integration from $t = 0$ to t, with the initial condition $g(0) = 1$ one obtains

$$g(t) = \frac{B/A}{(1 + B/A)(1 + t/t_a)^B - 1}$$

$$n_T(r, t) = \frac{n_T(0, 0)B/A}{[(1 + B/A)(1 + t/t_a)^B - 1](1 + t/t_a)} \exp\left[- \frac{r^2}{r_0^2(1 + t/t_a)} \right] \quad (20)$$

The conditions $A \leq 1$ and $B \ll 1$ were verified a posteriori by comparison with the experimental results, or using the parameter values of Table IB.

III.1.4 Resolution of equations (12) and (13) governing the singlet excitons evolution The light intensity is calculated by solving successively the four equations:

$$\frac{\partial n_S(r, t)}{\partial t} = D_S \nabla^2 n_S - \gamma_{SS} n_S^2 - \gamma_{ST} n_S n_T - k_S n_S + \gamma_S n_T^2 \quad (12)$$

$$N_S(t) = \int_0^r n_S(r, t) 2\pi r l dr \quad (21)$$

$$\frac{dN'_S(t)}{dt} = (1 - k'_S/k_S) k_S N_S(t) - k'_S N'_S(t) \quad (13)$$

$$i(t) = k'_S[N_S(t) + N'_S(t)] \quad (22)$$

These equations were solved numerically with a computer, using the parameter values of Table IA and $n_T(r, t)$ given by the Eq. (20). The parameter values were changed and the light intensity (22) calculated again, until the best fit was obtained between the calcdlated and *all experimental results*. These new values are reported in Table IB, and it can be seen that there is little difference compared to the previous values of Table IA.

III.2 Comparison to experimental results

III.2.1 Intensity decay of the scintillation The total number of singlet excitons in an anthracene crystal bombarded by a 5.3 MeV α particle, $N_S(t) + N'_S(t) = i(t)/k'_S$ is reported on the Figures 2 and 5. The full lines are the experimental results, and the broken line in Figure 2 and the crosses in Figure 5 are calculated values, using the fitted parameter values of the Table IB. On Figure 5 are also shown the calculated relative variations of the total number of triplet excitons $N_T(t)/N_T(0) = g(t)$.

The experimental curves $i(t)$ which were measured in Section II.1 and Section II.2 are only relative variations. Their normalization was calculated as follows: the scintillation yield of an anthracene crystal bombarded by

5.3 MeV α particles perpendicularly the crystal (a, b) plane is[34] $S_\alpha = 0.111\ S_\beta$ where S_β is the scintillation quantum yield for high energy β particle irradiation. Taking $S_\beta = 23$ photons/keV[6], one obtains: $S_\alpha = 2.55$ photons/keV, or 13000 emitted photons for one 5.3 MeV α particle. The normalization was achieved by integrating the experimental curve $i(t)$ and taking into account the relation $\int_0^\infty i(t)dt = 13000$ photons (see Figure 2 and 5).

Calculated and experimental results are quite similar, except at the beginning: the calculated initial spike corresponding to the very fast singlet excitons quenching by $S_1 - S_1$ or $S_1 - T_1$ interactions is washed out in the experimental results because the time resolution of the apparatus is too large (≈ 1 nsec).

As it was shown in Section II.2 and Figure 3, the initial singlet excitons quenching is more striking for naphtalene crystals. The reason of this difference between naphtalene and anthracene crystals is that in naphtalene all monomolecular or bimolecular rate constants, and the diffusion constants are about 10 times smaller than in anthracene: in naphtalene crystals $k'_S = 0.87 \times 10^7\ \text{sec}^{-1}$,[35] $k_S = 2.5 \times 10^7\ \text{sec}^{-1}$,[35] $D_S = 2 \times 10^{-5}\ \text{cm}^2\ \text{sec}^{-1}$,[36] $D_T = 3 \times 10^{-5}\ \text{cm}^2\ \text{sec}^{-1}$,[37,38] $\gamma_{TT} = 3 \times 10^{-12}\ \text{cm}^3\ \text{sec}^{-1}$.[37,39] Assuming a similar difference for γ_{SS} and γ_{ST}, it is clear that in naphtalene the variations with time of $N_S(t) + N'_S(t)$ are similar to those in anthracene, but slower by a factor of 10. Therefore, the initial quenching which is important during 1 nsec in anthracene will be important during 10 nsec in naphtalene and can be easily observed experimentally.

The quantitative description of the scintillation can give more information about some details of the excitons kinematics in the α particle track: Figure 10, curve 1 shows the calculated variations of $N_S(t) + N'_S(t)$ (using the fitted parameter values of the Table IB) which are quite the same as the experimental results. Curve 2 shows the scintillation prompt component which is given by the calculated values of $N_S(t) + N'_S(t)$, taking $\gamma_S = 0$ and γ_{TT} unchanged ($3.4 \times 10^{-11}\ \text{cm}^3/\text{sec}$).† Curve 3 shows the part of this prompt component which corresponds to the singlet excitons of the track ($N_S(t)$, taking the same condition $\gamma_S = 0$). From this curve it can be seen that the singlet excitons of the track, corresponding to the prompt component are quenched very quickly by bimolecular interaction; however, the radiative transition (rate constant k_S) which is a much slower process is not negligible. Among the photons arising from these singlet excitons of the track, 80% are self-absorbed out of the track and result in a quasi-exponential prompt component (curve 2), which time constant is $1/k'_S = 25$ nsec. The estrapolated value of the exponential curve to $t = 0$ is a good approximation to the

† In this calculation, the quenching of singlet excitons by those created by $T_1 - T_1$ annihilation is neglected compared to the quenching by triplet excitons which is much more efficient.

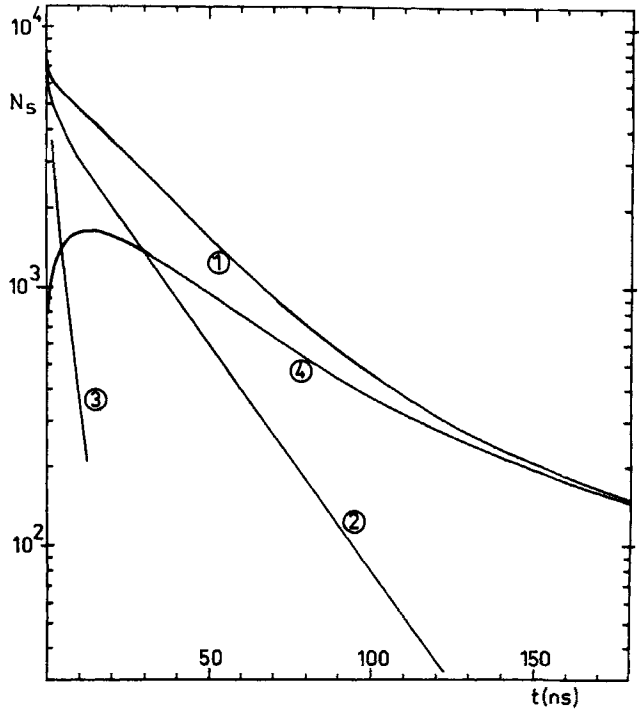

FIGURE 10 Time dependence of the number of singlet excitons in an anthracene crystal bombarded by a 5.3 MeV α particle.

1) Total number of singlet excitons ($N_S + N_S'$). Experimental and calculated values.
2) Calculated number of singlet excitons giving rise to the prompt component.
3) Calculated number of singlet excitons of the track giving rise to the prompt component.
4) Calculated number of singlet excitons giving rise to the delayed component.

number of singlet excitons, which result in the prompt component emission: 4900 excitons. The initial number of singlet excitons is 94000 (calculated with the parameter values of Table IB), and the ratio 4900/94000 $\approx$ 0.05 indicates that only 5 per cent of the initially created singlet excitons are not quenched by bimolecular processes. As the total number of emitted photons is 13000, the ratio of the prompt to the delayed component is P/D = 4900/(13000 − 4900) $\approx$ 0.6. This value is similar to the experimental value measured by Geacintov *et al.*,[4] but does not agree with the results of Schott who concluded that the prompt component is negligible.[3] The delayed component (curve 4) is the difference between curves 1 and 2.

On Figure 11 are reported the initial distributions of singlet and triplet excitons in the track (curve 1), calculated, taking the fitted parameter values

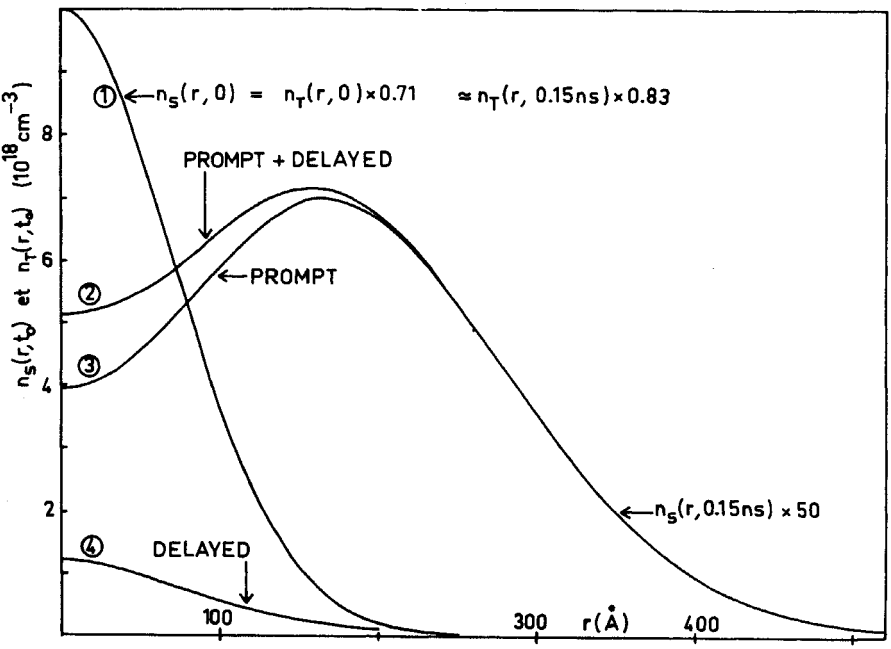

FIGURE 11 Calculated singlet ($n_S(r, t)$) and triplet ($n_T(r, t)$) excitons concentrations as a function of the distance to the center of the track in anthracene crystals bombarded by 5.3 MeV α particles perpendicularly to the crystal (a, b) plane.

of Table IB. Compared to the initial distribution, there is little difference in the triplet excitons concentrations after 0.15 nsec (curve 1), but the singlet excitons concentrations are completely changed (see curve 2). The part of these singlet excitons corresponding to the prompt component are shown by the curve 3, and the difference between the curves 2 and 3 correspond to the singlet excitons created by $T_1 - T_1$ annihilation (curve 4). From these results it can be seen that the singlet excitons of the track are very rapidly quenched, especially in the core of the track, by triplet excitons. The singlet excitons quenching by $S_1 - S_1$ interactions prevails at the beginning, but decreases very quickly, like the singlet concentrations, and becomes negligible compared to the quenching by triplet excitons: at 0.15 nsec and $r = 0$, $\gamma_{SS} n_S = 1.5 \times 10^{-8} \times 10^{17} = 1.5 \times 10^{9}\ \text{sec}^{-1}$ and $\gamma_{ST} n_T = 2 \times 10^{-9} \times 1.2 \times 10^{19} = 2.4 \times 10^{10}\ \text{sec}^{-1}$. Singlet excitons can only partly avoid quenching by diffusing out of the track: at 0.15 nsec and $r = 250$ Å,

$$\gamma_{ST} n_T = 2 \times 10^{-9} \times 4.4 \times 10^{16} \approx 10^{8}\ \text{sec}^{-1},$$

$$\gamma_{SS} n_S = 1.5 \times 10^{-8} \times 10^{17} = 1.5 \times 10^{9}\ \text{sec}^{-1}.$$

These singlet excitons annihilation rate constants are one order of magnitude smaller than at $r = 0$, but are still large compared to the rate constant of the radiative transition ($k_S = 2 \times 10^8$ sec^{-1}). Moreover, it is important to see that diffusion, which can get singlet excitons out of the track, has also the reverse effect: The diffusion length of a singlet exciton is $(D_S/k_S)^{1/2} \approx 500$ Å, therefore, at $t = 0.15$ nsec, the major part of the singlet excitons, which are less far than 500 Å from the track center will diffuse again to the center of the track where the quenching by triplet excitons is efficient. Another consequence of the singlet exciton diffusion is that in anthracene crystals the high energy secondary electrons, with lower LET, which create singlet excitons in regions with lower excitons concentrations will have an appreciable contribution to the scintillation yield only if their range is more than 500 Å, or their energy more than 1 keV.

The kinematics study can also account for the observed *temperature effect on the scintillation*. From Figure 6 and reference 40, it can be seen that the prompt component of the scintillation increases with decreasing temperatures. A quantitative comparison to the calculations is impossible because the variations of γ_{SS} and γ_{ST} with temperature are not known. However, the singlet exciton diffusion coefficient D_S decreases with increasing temperatures like $(T)^{-1/2}$,[36] and k_S is independent of the temperature;[27] assuming that γ_{SS} and γ_{ST} are nearly independent of temperature, it is easy to see, from Eq. (12) that at lower temperatures the singlet excitons quenching will be less efficient and the scintillation yield larger. In other words, at lower temperatures, the singlet exciton diffusion rate constant $(4D_S/r_0^2)$ becomes larger, compared to the quenching rate constants ($\gamma_{SS}n_S$ and $\gamma_{ST}n_T$). The opposite assumption, that the bimolecular reactions $S_1 - S_1$ and $S_1 - T_1$ are diffusion controlled,[41] or that γ_{SS} and γ_{ST} are proportional to D_S results (using the Eq. (12)) in a decrease of the scintillation yield with decreasing temperatures, which is not experimentally observed.

The kinematics study can also account for the experimentally observed *anisotropy of the scintillation yield* as a function of the direction of the α particle path in the crystal. The importance of the anisotropy in the beginning of the scintillation[40] suggests that, changing the orientation of the α particle path in the crystal, changes the rate constants of the singlet excitons diffusion out of the track, while the quenching rate constants $\gamma_{SS}n_S$ and $\gamma_{ST}n_T$ are unchanged. The prompt component intensity is the largest when the α particle path is perpendicular to the crystal (a, b) plane (direction c') because in that case the singlet excitons diffusion out of the track, in the (a, b) plane is the most efficient; this results in a minimum of the bimolecular quenching and a maximum of the prompt component intensity. The singlet excitons diffusion in the c' direction is slower because the intermolecular distance and intermolecular interactions are smaller in that direction. The prompt

omponent intensity is the lowest when the α particle path is parallel to the b xis;[42] if our theory is right one infers that the singlet excitons diffusion is the astest in the b direction. Therefore, the 3 components of the singlet excitons iffusion coefficient D_{Sa}, D_{Sb}, D_{Sc} in the directions a, b, c', are so that $D_{Sc} < D_{Sa} < D_{Sb}$. A similar experimental result was obtained for the triplet excitons diffusion coefficient,[21] and shows merely that intermolecular nteractions and excitation transfer are closely connected to the intermolecuar distances which are: $a = 8.58$ Å, $b = 6.02$ Å, $c = 11.8$ Å.

The anisotropy of the delayed component is governed by the triplet excions kinematics and is quite different from that of the prompt component. The experimental and theoretical problem was studied by Bönsch.[40]

III.2.2 Magnetic field effects The experimentally observed magnetic field effect on the scintillation of anthracene crystals bombarded by α particles (Section II.3) is unambiguously identified as a magnetic field effect on the $T_1 - T_1$ fusion reaction (Eq. 8). The effect being almost independent with time, shows that the delayed component is important, even in the beginning of the scintillation.

The reverse magnetic field effect on the prompt component with β particle irradiation,[9,18] which is an effect on the yield of the $T_1 + T_1$ excitons pair production (reaction 4) is not observed in the case of α particle irradiation. The reason for this is given in Section I.2. Therefore, we assume that in anthracene crystals excited by α particles the prompt component of the scintillation is not magnetic field sensitive.

The only two processes which can account for the magnetic field effect are the fusion $T_1 + T_1 \rightarrow S_0 + S_1$ and the triplet exciton quenching by doublets (spin $\frac{1}{2}$): see Section I.3. It is impossible to give a straightforward description of this problem, because the evolutions of the light intensity and of the singlet and triplet excitons concentrations are given by complicated functions of γ_S and γ_R. Therefore, the Eqs. (19), (12), (21), (13), (22) were solved, using the same methods as previously (Section III.1.3 and III.1.4), and the light intensity $i(t)$ was calculated in various magnetic field conditions, i.e. with various values of γ_S and γ_R, whose variations with the magnetic field are well known.[14,15,20] The calculated light intensity was then integrated between 0 and 80 nsec (i_p value) and between 0.7 μsec and 10 μsec (i_d value). The relative variations of the integrated intensities $\Delta i_p/i_p = (i_p(\mathbf{H}) - i_p(0))/i_p(0)$ and $\Delta i_d/i_d$ resulting from the application of a magnetic field, were then calculated and compared to the experimental results: see Figure 9. The best fit was obtained using the parameter values of Table IB and the variations of $\gamma_S(\mathbf{H})$ and $\gamma_R(\mathbf{H})$ given in the Refs. 14, 15 and 20. It should be said, as in Section III.1.4, that this fitting and the fitting of $i(t)$ were achieved simultaneously for the determination of the parameter values of the Table IB.

It can be seen that the variations $\Delta i_p/i_p$ result almost exclusively from the variations $\Delta\gamma_S/\gamma_S$ of $\gamma_S(\mathbf{H})$: $\Delta i_p/i_p$ is proportionnal to $\Delta\gamma_S/\gamma_S$. However $|\Delta i_p/i_p| < |\Delta\gamma_S/\gamma_S|$ for two reasons: the first one is that only a fraction of the light originates from $T_1 - T_1$ annihilation (see Figure 10), whereas the prompt component is not magnetic field dependent. The second reason is that at high triplet exciton densities, the variation of $\gamma_S(\mathbf{H})$ results in a reverse variation of the triplet excitons concentration and a decrease of the magnetic field effect.[26] In this time scale (0 to 80 nsec) the triplet excitons concentration and the light intensity are not significantly changed by the triplet excitons quenching by radicals, which is too slow and the influence of $\Delta\gamma_R/\gamma_R$ is negligible.

This is not the case at longer time scales. The variation $\Delta i_d/i_d$ are not proportionnal to $\Delta\gamma_S/\gamma_S$. At $|\mathbf{H}| = 420$ Gauss, in a resonance direction of the (a, b) plane, $\Delta\gamma_S/\gamma_S = 0$, whereas $\Delta i_d/i_d = 0.6$ per cent. If only the γ_S variations are taken into account, the calculated variations $\Delta i_d/i_d$ are always below the experimental values. This difference increases monotonically with the magnetic field intensity, because the quenching of triplet excitons by radicals is slower when a magnetic field is applied. Therefore, $\Delta\gamma_R/\gamma_R$ cannot be neglected here.

References

1. T. A. King and R. Voltz, *Proc. Roy. Soc. A*, **289**, 424 (1966).
2. R. Voltz, International Discussion on Progress and Problems in Contemporary Radiation Chemistry, Proceedings of the 30th Czechoslovak Annual Meeting (1970).
3. M. Schott, Thesis, Paris (1972).
4. N. E. Geacintov, M. Binder, C. E. Swenberg, and M. Pope, *Phys. Rev.*, **B12**, 4113 (1975).
5. H. Venghaus, *Z. Phys.*, **239**, 289 (1970).
6. T. R. Fisher and D. Kohler, *Rev. Scient. Instr.*, **43**, 471 (1972).
7. G. Klein and R. Voltz, in *Molecular Spectroscopy of Dense Phases*, Proceedings of the 12th European Congress on Molecular Spectroscopy, Elsevier, Amsterdam (1976).
8. C. Fuchs, F. Heisel and R. Voltz, *J. Phys. Chem.*, **76**, 3867 (1972).
9. G. Klein, Thesis, Strasbourg (1977).
10. M. Silver and R. Sharma, *J. Chem. Phys.*, **46**, 692 (1967).
11. R. R. Chance and C. L. Braun, *J. Chem. Phys.*, **64**, 3573 (1976).
12. N. Wakayama and D. F. Williams, *J. Chem. Phys.*, **57**, 1770 (1972).
13. M. Schott and J. Berrehar, *Mol. Cryst. Liq. Cryst.*, **20**, 13 (1973).
14. V. Ern and R. E. Merrifield, *Phys. Rev. Let.*, **21**, 609 (1968).
15. V. Ern and A. R. McGhie, *Mol. Cryst. Liq. Cryst.*, **15**, 277 (1971).
16. W. G. Burns and J. D. Jones, *Trans. Farad. Soc.*, **60**, 2022 (1964).
17. G. T. Wright, *Proc. Phys. Soc.*, **B68**, 701 (1955).
18. G. Klein and R. Voltz, Sixth Molecular Crystal Symposium, Schloss Elmau (1973).
19. P. Avakian, *Pure Appl. Chem.*, **37**, 1 (1974).
20. R. C. Johnson and R. E. Merrifield, *Phys. Rev.* **B1**, 896 (1970).
21. V. Ern, *Phys. Rev. Let.*, **22**, 343 (1969).
22. R. C. Powell and Z. G. Soos, *J. Luminescence*, **11**, 1 (1975).
23. J. Fourny, M. Schott, and G. Delacote, *Chem. Phys. Lett.*, **20**, 559 (1973).
24. S. D. Babenko, V. A. Benderskii, V. I. Goldanskii, A. G. Lavrushko, and V. P. Tychinskii, *Phys. Sat. Sol.* (b), **45**, 91 (1971).

25. P. Avakian and R. E. Merrifield, *Mol. Cryst. Liq. Cryst.*, **5**, 37 (1968).
26. R. P. Groff, R. E. Merrifield, and P. Avakian, *Chem. Phys. Let.*, **5**, 168 (1970).
27. I. H. Munro, L. M. Logan, F. D. Blair, F. R. Lipsett, and D. F. Williams, *Mol. Cryst. Liq. Cryst.*, **15**, 297 (1972).
28. I. Nakada, *J. Phys. Soc. Japan*, **20**, 346 (1965).
29. J. A. Miehé, G. Ambard, J. Zampach, and A. Coche, *IEEE Trans. Nucl. Sc.*, **NS-17**, 3, 115 (1970); L. M. Bolinger and G. E. Thomas, *Rev. Scient. Instr.*, **32**, 1044 (1961).
30. Unpublished.
31. J. L. Da Silva, Thesis, Strasbourg (1969); R. Voltz, J. L. Da Silva, G. Laustriat, and A. Coche, *J. Chem. Phys.*, **45**, 3306 (1966).
32. S. Owaki, Y. Kimura, M. Kawanishi, and K. Sugihara, *J. Phys. Soc. Japan*, **28**, 691 (1970).
33. A. Kuppermann and G. G. Belford, *J. Chem. Phys.*, **36**, 1412 (1962).
34. M. Schumacher and A. Flammersfeld, *Z. Phys.*, **178**, 11 (1964).
35. T. B. El Kareh and H. C. Wolf, *Mol. Cryst. Liq. Cryst.*, **4**, 195 (1968).
36. A. Hammer and H. C. Wolf, *Mol. Cryst. Liq. Cryst.*, **4**, 191 (1968).
37. C. E. Swenberg, *J. Chem. Phys.*, **51**, 1753 (1969).
38. V. Ern, *J. Chem. Phys.*, **56**, 6259 (1972).
39. K. W. Benz, H. Port, and H. C. Wolf, *Z. Naturforsch.*, **26a**, 787 (1971).
40. G. Bönsch, *Z. Physik*, **212**, 497 (1968).
41. A. Bergman, D. Bergman, and J. Jortner, *Israël J. Chem.*, **10**, 471 (1972).
42. W. F. Kienzle and A. Flammersfeld, *Z. Phys.*, **165**, 1 (1961).
43. J. B. Birks, *The Theory and Practice of Scintillation Counting*, Pergamon, Oxford (1964).